MINISTRY OF EDUCATION AND TRAINING
HCMC UNIVERSITY OF TECHNOLOGY AND EDUCATION

DAO THI THU THUY

DESIGN AND ANALYZE THE PROTOCOLS TO ENHANCE THE PERFORMANCE OF THE TWO-WAY COOPERATION NETWORKS.

Major: Electronic Engineering
Major code: 9520203

SUMMARY OF PH.D. THESIS

HO CHI MINH CITY – 2023

This thesis was completed at HCMC University of Technology and Education

Supervisor: Dr. Pham Ngoc Son

Reviewer 1:
Reviewer 2:
Reviewer 3:

The dissertation was presented at the primary committee of at Faculty of Electrical and Electronics Engineering, HCMC University of Technology and Education, 2023.

PUBLICATIONS

[P1]. **Thu-Thuy Thi Dao**, Pham Ngoc Sơn "Uplink Non-Orthogonal Multiple Access Protocol in Two-Way Relaying Networks: Realistic Operation and Performance Analysis," *2020 7th NAFOSTED Conference on Information and Computer Science (NICS)*, VNUHCM, Vietnam 11/2020 (IEEE Xplore).

[P2]. **Thu-Thuy Thi Dao,** Pham Ngoc Son, "Cancel-Decode-Encode Processing on Two-Way Cooperative NOMA Schemes in Realistic Conditions," *Wireless Communications and Mobile Computing*, vol 2021, Article ID 8828443, 15 pages, 2021 (SCIE).

[P3]. **Thu-Thuy Thi Dao, Pham Ngoc Sơn "Two-Way Cognitive Network** supported by Reconfigurable Intelligent Surface," *2021 International Conference on Advanced Technologies for Communications (2021ATC)*, Ho Chi Minh city, Vietnam. 10/2021 (IEEE Xplore).

[P4]. **Thu-Thuy Thi Dao**, Pham Ngoc Sơn "Multi-constraint two-way underlay cognitive network using, reconfigurable intelligent surface," *Wireless Networks*, 2022/04/06 2022 (SCIE).

[P5]. **Thu-Thuy Thi Dao**, Pham Ngoc Sơn "Performance analysis of two-way network with nonlinear energy harvesting relay and digital network coding," *The 2nd International Conference on Advanced Technology and Sustainable Development – 2022 (ICATSD 2022)*, Ho Chi Minh city, Vietnam, 11/2022.

INTRODUCTION

1. Research Reasons.

Nowadays, with the remarkable development of science and technology, the fourth industrial revolution, and the widespread use of IoT technology, the number of users and wireless-connected devices is rapidly increasing. Along with this, the amount of data circulating over wireless environments is also growing at an exponential rate. This presents numerous challenges for wireless communication networks, such as efficient energy utilization or energy saving, efficient spectrum utilization, capacity enhancement, data rate improvement, latency reduction, and service quality enhancement. Two-way cooperative wireless networks can address these challenges by offering high spatial diversity, mitigating the effects of transmission fading, improving network access throughput, and enhancing coverage quality compared to direct transmission networks. In addition, cognitive radio technology helps improve spectrum utilization efficiency by allowing secondary network devices to share the licensed spectrum of primary users. Recently, the research on reconfigurable intelligent surface, also known as smart reflecting surface, has brought benefits such as increased spectrum efficiency, energy savings, and reduced initial investment costs.

For researching solutions to meet the practical requirements of wireless networks, the dissertation title "**Design and analysis of protocols for enhancing performance in two-way cooperative networks**" was selected to be implemented.

2. Research Objectives and Contents

Designing new models and protocols to enhance system performance of two-way cooperative networks in both conventional wireless and cognitive wireless environments.

Analyzing the performance evaluation criteria of the proposed protocols using explicit mathematical expressions, approximate mathematical expressions, or asymptotic expressions.

The thesis examines models under more realistic assumptions than existing works, such as imperfect channel state information acquisition, imperfect successive interference cancellation conditions, the presence of residual loops after interference cancellation at the full-duplex receivers, and nonlinear energy harvesting.

3. Research Object and Scope

Two-way cooperative network, two-way cognitive radio network, network performance evaluation criteria such as outage probability, throughput.

Techniques to improve two-way system performance: digital network coding; relay selections; nonorthogonal multiple access; successive interference cancellation; radio energy harvesting; full-duplex transmission.

Using an emerging cost-saving technology is the reconfigurable intelligent surface in the two-way network.

Realistic constraints, and Rayleigh fading channels have the same distribution and are independent.

4. Research's Scientific and Practical Significance

Proposing a solution that combines digital network coding successive interference cancellation, and relay clusters to reduce signal transmission time, increase the likelihood of successful signal transmission, and increase throughput for the two-way network. In addition, considering the system under more realistic assumptions such as imperfect channel state information and imperfect successive interference cancellation.

Proposing a reconfigurable intelligent surface supported underlay two-way scheme operating in sub-6GHz bands to enhance the spectral efficiency, the energy-efficiency, and the cost-efficiency. The model has been analyzed under the actual condition that existing the residual loop-back interference in the

receiving antenna of two secondary sources due to the full-duplex mode and the secondary network is power-limited due to multiple primary receivers.

Using energy harvesting via radio signals to support low-cost and resource-constrained two-way cooperative radio networks such as wireless sensor networks and IoT networks. And the model also is considered in the real condition that the electronic components of the energy-collecting device of the relay have a nonlinear character.

Chapter 1. OVERVIEW OF THE RESEARCH

In this chapter, the publications related to enhance performance of the two-way radio networks and two-way cooperative radio networks in recent years are analyzed, synthesized, and compared. Afterward, outstanding issues and issues that can be developed are identified then the research directions of the thesis are proposed.

Chapter 2. FUNDAMENTAL THEORY

In this chapter, the theoretical basis of TW cooperative radio network models and radio channel models are presented briefly. The chapter also presents the technologies which are used in the next chapters such as the digital network coding, the relay selection, the nonorthogonal multiple access, successive interference cancellation, the cooperative radio, and the energy harvesting.

## Chapter 3. TWO-WAY COOPERATIVE NETWORK USING SUCCESSIVE INTERFERENCE CANCELLATION AND DIGITAL NETWORK CODING

3.1 Introduction

In this chapter, the PhD student proposes a two-way cooperative network model consisting of two sources and a relay cluster to increase the system throughput and reduce the outage probability. The model uses a combination of successive interference cancellation (SIC), digital network coding (DNC) and partial relay

selection techniques. The model has two time slots (TS) for signal transmission (called as the SIC-2TS protocol) and operates in half-duplex mode. The system throughput and outage probabilities are considered under the conditions of perfect/imperfect SIC (pSIC/ipSIC) and perfect/imperfect channel state information (pCSI/ipCSI).

The contribution of chapter 3 is presented in the publication [P2]

3.2 System model
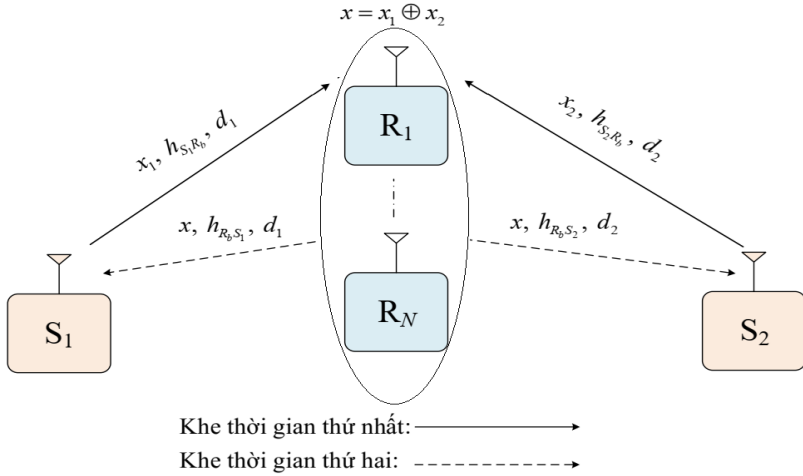
Figure 0.0: *System model SIC-2TS.*

A cooperative two-way network model has two sources S_1, S_2 and a closed group of N relay R_i, with $i \in \{1, 2, ... N\}$ as figure 3.1.

3.3 Signal transmission and signal-to-noise ratio

The signal which the relays receive in the first time slot is:

$$y_{R_i} = \sqrt{\alpha_1 P_S} h_{S_1 R_i} x_1 + \sqrt{\alpha_2 P_S} h_{S_2 R_i} x_2 + n_{R_i}.$$ (3.1)

Due to ipCSI condition, the estimated channel coefficient $\hat{h}_f$ is presented by the channel coefficient h_f as:

$$\hat{h}_f = \rho_f h_f + \left(\sqrt{1 - \rho_f^2}\right)\varepsilon_f$$ (3.2)

SINR for detecting the signal x_n of the near source S_n at relays is given by:

$$\gamma_{S_n R_i \to x_n | d_n \le d_d} = \frac{\alpha_n \left| \hat{h}_{S_n R_i} \right|^2}{\alpha_d \left| \hat{h}_{S_d R_i} \right|^2 + \left(\alpha_n \lambda_n + \alpha_d \lambda_d \right) \left(1 - \rho^2 \right) + \rho^2 / \gamma}. \tag{3.6}$$

The relay R_b is selected in MAC layer protocol so that maximizing estimated channel gains to enhance the decoding capacity of the nearer source signal and minimize the collection time of imperfect CSI:

$$R_b = \arg \max_{i=1\ldots N} g_{S_n R_i} \tag{3.7}$$

SINR for detecting the signal x_d of the far source S_d at relay R_b is given by:

$$\gamma_{S_d R_b \to x_d | d_n \le d_d} = \frac{\alpha_d \left| \hat{h}_{S_d R_b} \right|^2}{\varepsilon \left| h_{R_b} \right|^2 \rho^2 + \left(\alpha_n \lambda_n + \alpha_d \lambda_d \right) \left(1 - \rho^2 \right) + \rho^2 / \gamma}. \tag{3.8}$$

In the second time slot, at the relay R_b, the signal $x = x_1 \oplus x_2$ is synthesized and transmitted to two sources. The x signal is detected with the SINR as follows:

$$\gamma_{R_b S_k \to x} = \frac{P_R \left| \hat{h}_{R_b S_k} \right|^2 / \rho^2}{P_R \lambda_k \left(1 - \rho^2 \right) / \rho^2 + N_0} = \frac{\eta \gamma g_{R_b S_k}}{\eta \gamma \lambda_k \left(1 - \rho^2 \right) + \rho^2}. \tag{3.10}$$

3.4 Performance analysis

3.4.1 Outage probabilities in the SIC-2TS protocol

The outage probability at the far source S_d is obtained as:

$$\text{OP}_{S_d} \Big|_{d_n \le d_d} = 1 - \left(1 - \lambda_n \sum_{p=0}^{N} \frac{C_N^p (-1)^p e^{-p\phi_3 / \lambda_n}}{\lambda_n + p\phi_2 \lambda_d} \right) \left(e^{-\gamma_t \left((1-\rho^2) + \rho^2 / (\lambda_d \eta \gamma) \right)} \right). \tag{3.16}$$

The outage probability at the near source S_n is obtained as:

$$
\left. OP_{S_n} \right|_{d_n \leq d_d} = 1 - \left(\begin{array}{l} \dfrac{\lambda_d e^{-\phi_5/\lambda_d}}{(\lambda_d + \phi_4 \Omega)} - \\[2mm] - \displaystyle\sum_{p=0}^{N} \dfrac{\lambda_n^{\,2} \lambda_d C_N^p (-1)^p e^{-(p(\phi_3 + \phi_5 \phi_2)/\lambda_n + \phi_5/\lambda_d)}}{(\lambda_n + p\phi_2 \lambda_d)(\lambda_n \lambda_d + \phi_4 \Omega(\lambda_n + p\phi_5 \phi_2 \lambda_d))} \end{array} \right) \times
$$

$$
\times \left(e^{-\gamma_t \left((1-\rho^2) + \rho^2/(\lambda_n \gamma) \right)} \right). \tag{3.18}
$$

When $\gamma \to +\infty$, we obtain asymptotic expression as:

$$
\left. OP_{S_d} \right|_{d_n \leq d_d}^{\gamma \to +\infty} = 1 - \left(1 - \lambda_n \sum_{p=0}^{N} \frac{C_N^p (-1)^p e^{-p\phi_6/\lambda_n}}{\lambda_n + p\phi_2 \lambda_d} \right) e^{-\gamma_t (1-\rho^2)}, \tag{3.19}
$$

$$
\left. OP_{S_n} \right|_{d_n \leq d_d}^{\gamma \to +\infty} = 1 - \left(\begin{array}{l} \dfrac{\lambda_d e^{-\phi_7/\lambda_d}}{(\lambda_d + \phi_4 \Omega)} - \\[2mm] \displaystyle\sum_{p=0}^{N} \dfrac{\lambda_n^{\,2} \lambda_d C_N^p (-1)^p e^{-(p(\phi_6 + \phi_7 \phi_2)/\lambda_n + \phi_7/\lambda_d)}}{(\lambda_n + p\phi_2 \lambda_d)(\lambda_n \lambda_d + \phi_4 \Omega(\lambda_n + p\phi_7 \phi_2 \lambda_d))} \end{array} \right) e^{-\gamma_t (1-\rho^2)}. \tag{3.20}
$$

3.4.2 Outage probabilities in the SIC-3TS and SIC-4TS protocols

To highlight the advantages of the proposed protocol, the author compares the proposed protocol with two others of the model: the first protocol use SIC technique but not using DNC technique (called as the SIC-3TS protocol); the second protocol without use both SIC and DNC techniques (called as the CONV-4TS protocol).

The outage probabilities of two sources in the SIC-3TS protocol are the same as the proposed SIC_2TS protocol. The outage probabilities of two sources in the SIC-4TS protocol are obtained as:

$$
OP_{S_2}^C = 1 - \left(1 - \sum_{p=0}^{N} C_N^p (-1)^p e^{-p\phi_8/\lambda_1} \right) e^{-\phi_9/\lambda_2}, \tag{3.21}
$$

$$
OP_{S_1}^C = 1 - \left(1 - \sum_{p=0}^{N} C_N^p (-1)^p e^{-p\phi_{10}/\lambda_1} \right) e^{-\phi_{11}/\lambda_2}. \tag{3.22}
$$

When $\gamma \to +\infty$, we obtain asymptotic expression as:

$$
\left. OP_{S_2}^C \right|_{\gamma \to +\infty} = 1 - \left(1 - \sum_{p=0}^{N} C_N^p (-1)^p e^{-p\gamma_t (1-\rho^2)} \right) e^{-\gamma_t (1-\rho^2)}, \tag{3.23}
$$

$$\left.\text{OP}_{S_1}^{C}\right|_{\gamma \to +\infty} = 1 - \left(1 - \sum_{p=0}^{N} C_N^p (-1)^p e^{-p\gamma_t\left(1-\rho^2\right)}\right) e^{-\gamma_t\left(1-\rho^2\right)}. \tag{3.24}$$

3.4.3   System throughput of three protocols

$$\left.\text{TP}_{\text{SIC-2TS}}\right|_{d_n \le d_d} = \frac{1}{2}\left(1 - \left.\text{OP}_{S_n}\right|_{d_n \le d_d}\right)R_t + \frac{1}{2}\left(1 - \left.\text{OP}_{S_d}\right|_{d_n \le d_d}\right)R_t,$$

$$\left.\text{TP}_{\text{SIC-3TS}}\right|_{d_n \le d_d} = \frac{1}{3}\left(1 - \left.\text{OP}_{S_n}\right|_{d_n \le d_d}\right)R_t + \frac{1}{3}\left(1 - \left.\text{OP}_{S_d}\right|_{d_n \le d_d}\right)R_t, \tag{3.26}$$

$$\text{TP}_{\text{CONV-4TS}} = \frac{1}{4}\left(1 - \text{OP}_{S_1}^{C}\right)R_t + \frac{1}{4}\left(1 - \text{OP}_{S_2}^{C}\right)R_t.$$
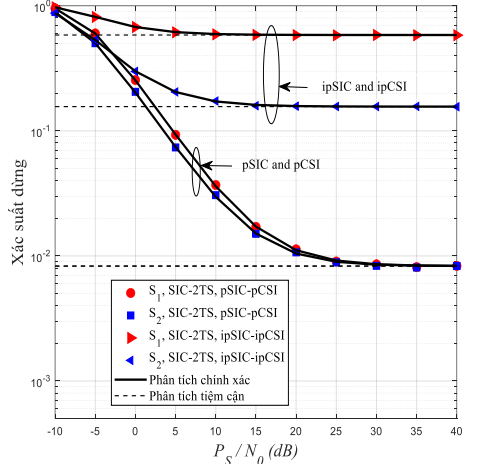
3.5 Simulation and discussion

From Figures 3.2 to 3.5, supposing that S_1 is nearer the relay cluster than S_2.

Fig 3.2 shows the OPs of two sources of the SIC-2TS protocol versus $P_S / N_0 (dB)$ with pCSI and pSIC/ipSIC. The results show that the outage
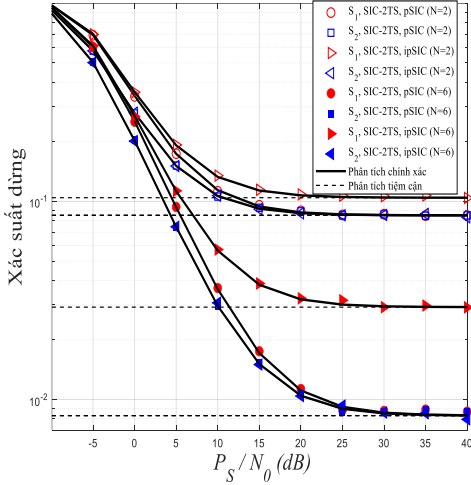
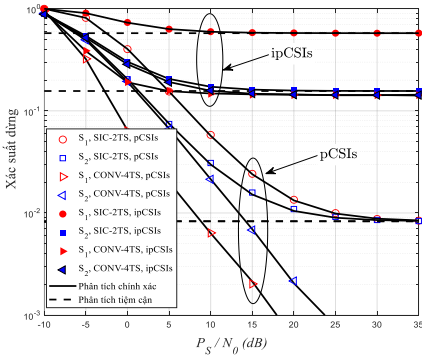**Figure 3.2:** OP_{S_1} *and* OP_{S_2} *of SIC-2TS when pSIC and ipSIC.*

Figure 3.3: OP_{S_1} *and* OP_{S_2} *of SIC-2TS when pSIC- pCSIs and ipSIC-ipCSIs.*

probabilities (OP) of both sources decrease as the $P_S / N_0 (dB)$ increases and reach a saturation value when $P_S / N_0 (dB)$ becomes sufficiently large. The OPs of the source S_2 are equal in the pSIC case and the ipSIC case. The OPs of

the source S_1 in the ipSIC case are higher than those in the pSIC. The OPs of the two sources decrease as the number of relays increases.

Fig 3.3 shows the OPs of two sources in the SIC-2TS protocol versus $P_S / N_0 (dB)$ in the two cases pSIC- pCSIs and ipSIC- ipCSIs. The OPs of the two sources with the pSIC- pCSI condition are better than with the ipSIC-ipCSI condition. In the ipSIC-ipCSI case, the OPs for the source S_1 are a lot higher. In order to have fairness between the sources, we can change the transmit power factor to the OPs of the two sources can be approximately equal.

Fig 3.4 shows the OPs of two sources in the SIC-2TS and CONV-4TS protocols versus $P_S / N_0 (dB)$ with pSIC and the two cases pCSIs/ipCSIs. The results show that the OPs of CONV-4TS protocol have lower than those of SIC-2TS protocol in both pCSIs and ipCSIs, because the transmission of each signal is simpler. However, the difference between the OPs of the two protocols decreases in case ipCSIs.
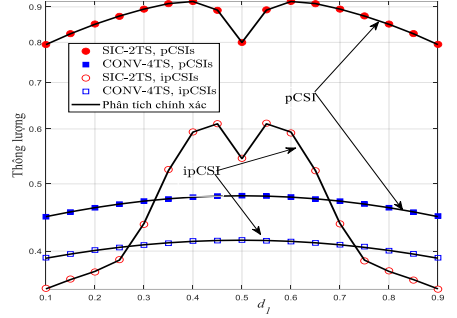

Figure 3.4: OP_{S_1} *and* OP_{S_2} *of SIC-2TS and CONV-4TS* when *pCSIs and*
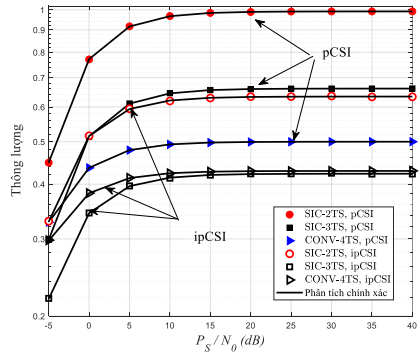
**Figure 3.5:** TP *of SIC-2TS, CONV-4TS and SIC-3TS when CSI and ipCSI.*

Fig 3.5 shows the system throughput(TP) of the SIC-2TS, CONV-4TS and SIC-3TS protocols in two cases pCSI and ipCSI. The TP of the SIC-2TS protocol is superior to the other two protocols in both pCSI and ipCSI. The TP of all three protocols in the pCSI case is always better than the ipCSI case, and the TP of all protocols reach saturation when $P_S / N_0 (dB)$ is a sufficiently large value.

Figure 3.6 shows the TP of SIC-2TS and CONV-4TS versus d_1. The results show that the TP of SIC-2TS protocol outperforms the TP of CONV-4TS in pCSIs case. In ipCSIs, the TP of the SIC-2TS protocol is only higher than the TP of the CONV-4TS protocol in the range of d_1 from 0.3 to 0.7. The TP of the SIC-2TS protocol has the highest value at $d_1 = \{0.4, 0.6\}$ (with pCSIs) and $d_1 = \{0.45, 0.55\}$ (with ipCSIs).

Figure 3.6: *TP of SIC-2TS and CONV-4TS versus d_1.*

The CONV-4TS protocol has the highest TP when the relay device is equidistant from the two sources.

Figure 3.7 shows the TP of the SIC-2TS protocol versus α_1 and d_1. The results show that the TP of the SIC-2TS protocol reaches maximum at about 0.885 when $\{\alpha_1, d_1\} = \{0.4, 0.5\}$ and $\{\alpha_1, d_1\} = \{0.6, 0.5\}$. With a reasonable allocation of transmit power, the best TP for the SIC-2TS protocol can be achieved. (Table 3.1).
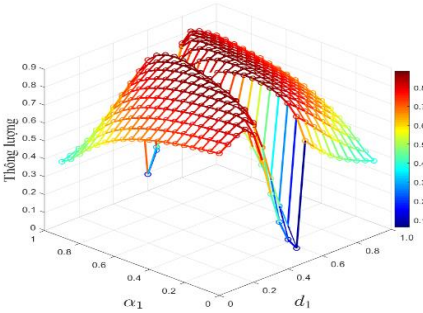
Figure 3.7: *TP* of *SIC-2TS versus α_1 and d_1.*
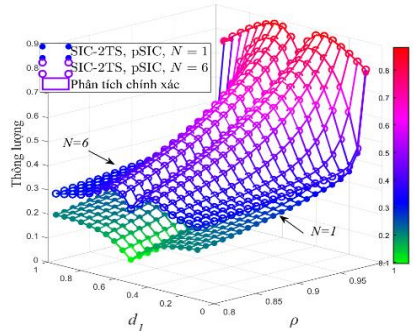
Figure 3.8: TP *of SIC-2TS versus d_1 and ρ.*

Figure 3.8 shows the system throughput of the SIC-2TS protocol versus d_1 and ρ. We can see that a small change in ρ will lead to a large change in TP. Besides, the relative distance between the two sources and the relay cluster also

differently affects the change of the TP when ρ decreases. And if the number of relays increases, the TP increases.

Finally, the analysis lines of all the figures coincide with the simulation lines.

Table 3.1: *The maximum throughput at each value of d_1 and α_1.*

d_1	0.1	0.2	0.3	0.4	0.5	0.6	0.7	0.8	0.9
α_1	0.1	0.1	0.3	0.5	0.3	0.5	0.7	0.9	0.9
TP_{max}	0.7839	0.8413	0.8715	0.8853	0.8754	0.8853	0.8715	0.8413	0.7839

3.6 Conclusion

Based on the analysis of outage probability and throughput, some of the main conclusions of the two-way cooperative network model with the proposed protocol SIC-2TS are as follows: The throughput of the SIC-2TS protocol is superior to the CONV-4TS and SIC-3TS protocols. System performance in ipSIC/ipCSI cases is always lower than ideal pSIC/pCSI cases. As the number of relays in the cluster increases, the system performance increases. The proposed relay selection method minimizes the collection time of ipCSIs compared to other RS methods. The SIC-2TS protocol can achieve the best performance at the optimal locations of the relay and the appropriate power division factor for the two sources.

Chapter 4. TWO-WAY COGNITIVE RADIO USING RECONFIGURABLE INTELLIGENT SURFACE

4.1 Introduction

In this chapter, a two-way cooperative cognitive radio network model with the support of reconfigurable intelligent surface is studied for communication. RIS is a new communications support solution that saves deployment costs, saves energy, and cognitive radio technology improves spectrum efficiency. The model considers the fact that there is still loop interference in the receiving antennas of the two secondary sources due to FD mode.
The contribution of chapter 4 is presented in the publication [P4].

4.2 System model
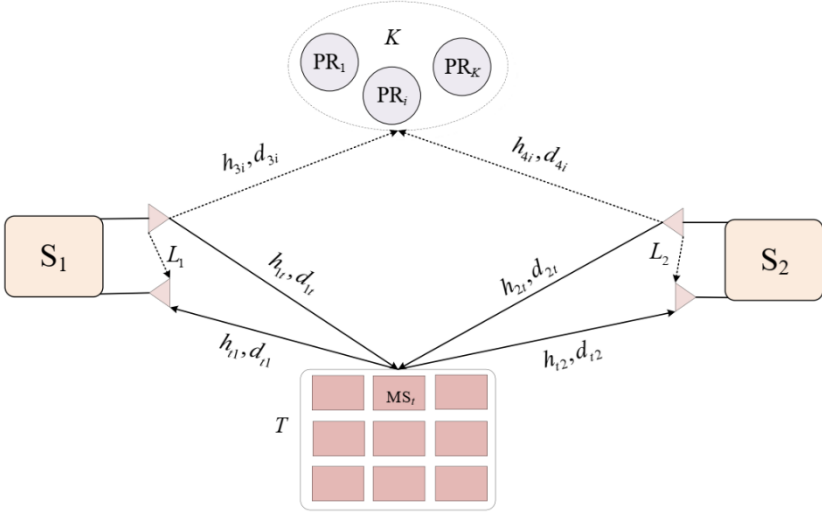
Figure 4.1: *System model MPR-UTW-RIS*

Figure 4.1 is a model of an underlay two-way cognitive radio network consisting of: two secondary sources S_q with $q \in \{1,2\}$, a RIS with T reflectors MS_t with $t = \{1,2,...,T\}$ and K primary receivers PR_i with $i = \{1,2,...,K\}$. The two secondary sources are subject to a transmit power limit such that the interference constraint to the devices PR_i must be less than a given threshold level I_i to ensure that primary network operations are not affected. The system operates in FD mode.

4.3 Signal transmission and signal-to-noise ratio

The signal which the source S_1 receives as:

$$y_1 = \underbrace{\sqrt{P_2}\, x_2 \left(\sum_{t=1}^{T} h_{2t} r_t h_{t1} \right)}_{\text{Desired signal}} + \underbrace{\sqrt{P_1}\, x_1 \left(\sum_{t=1}^{T} h_{1t} r_t h_{t1} \right)}_{\text{Self-inteference signal}} + L_1 + n_1. \qquad (4.2)$$

Assuming S_1 is possible to completely suppress the self-interference signal and optimize the phase of MS_t $\phi_t = -(\varphi_{1t} + \varphi_{2t})$.

$$y_1 = \sqrt{P_2}\, x_2 \left(\sum_{t=1}^{T} |h_{2t}| \times |h_{t1}| \right) + L_1 + n_1. \qquad (4.3)$$

11

SINR for detecting the signal at S_1:

$$\gamma_1 = \min(\gamma_0, \frac{Q}{\max\limits_{i=1...K} g_{4i}}) \frac{\Psi^2}{(1+\mu_1)}. \tag{4.5}$$

SINR for detecting the signal at S_2:

$$\gamma_2 = \min(\gamma_0, \frac{Q}{\max\limits_{i=1...K} g_{3i}}) \frac{\Psi^2}{(1+\mu_2)}. \tag{4.8}$$

4.4 Performance analysis

In this section, the OPs of two secondary sources S_p and S_w, ($p, w = \{1,2\}$ and $p \neq w$) are analyzed. The outage probabilities at S_p in the integral expression (4.22) and the infinite sum expression (4.23):

$$\mathrm{OP}_{S_p}^{out} = \frac{\left(a+1,(1/b)\sqrt{\alpha_1/\gamma_0}\right)}{\Gamma(a+1)} \left(1 - e^{-\lambda_{(w+2)}Q/\gamma_0}\right)^K + K\left(\alpha_2/\left(2b\sqrt{\lambda_{(w+2)}}\right)\right)^{(a+1/2)} \times$$

$$\times \sum_{m=0}^{K-1} C_{K-1}^m (-1)^m (m+1)^{-(a+5/2)/2} e^{\left(\alpha_2^2/\left(8b^2\lambda_{(w+2)}(m+1)\right)\right)} W_{-\frac{(a+1/2)}{2},-\frac{1}{4}\left(\alpha_2^2/\left(4b^2\lambda_{(w+2)}(m+1)\right)\right)} - \tag{4.22}$$

$$-(1 - e^{-\lambda_{(w+2)}\alpha_3})^K + \int_0^{\alpha_3} K\lambda_{(w+2)} \left(1 - e^{-\lambda_{(w+2)}x}\right)^{K-1} e^{-\lambda_{(w+2)}x} \frac{\Gamma\left(a+1,(\alpha_2/b)\sqrt{x}\right)}{\Gamma(a+1)} dx.$$

$$\mathrm{OP}_{S_p}^{out} = \frac{\gamma\left(a+1,(1/b)\sqrt{\alpha_1/\gamma_0}\right)}{\Gamma(a+1)} \left(1 - e^{-\lambda_{(w+2)}Q/\gamma_0}\right)^K + K\left(\frac{\alpha_2}{2b\sqrt{\lambda_{(w+2)}}}\right)^{(a+1/2)} \times$$

$$\times \sum_{m=0}^{K-1} C_{K-1}^m (-1)^m (m+1)^{-\frac{1}{2}\left(a+\frac{5}{2}\right)} e^{\left(\frac{\alpha_2^2}{8b^2\lambda_{(w+2)}(m+1)}\right)} W_{-\frac{1}{2}(a+1/2),-\frac{1}{4}\left(\alpha_2^2/\left(4b^2\lambda_{(w+2)}(m+1)\right)\right)} - \tag{4.23}$$

$$-\frac{K\lambda_{(w+2)}}{\Gamma(a+1)} \sum_{n=0}^{\infty} \frac{(-1)^n}{n!(a+1+n)} \sum_{m=0}^{K-1} C_{K-1}^m (-1)^m \left(\lambda_{(w+2)}(m+1)\right)^{-((1/2)(a+1+n)+1)} \times$$

$$\times \gamma\left((1/2)(a+1+n)+1, \lambda_{(w+2)}(m+1)\alpha_3\right).$$

The infinite sum expression in (4.23) can be evaluated for accuracy by the error metric as:

$$\xi_p = \left(\left|\mathrm{OP}_{S_p}^{out}(4.22) - \mathrm{OP}_{S_p}^{out}(4.23)\right|\right) / \left(\mathrm{OP}_{S_p}^{out}(4.22)\right). \tag{4.24}$$

The asymptotic expression as $\gamma_0 \to +\infty$:

$$\text{OP}_{S_p}^{out,\gamma_0\to\infty} = \zeta_1 = K\left(\frac{\alpha_2}{2b\sqrt{\lambda_{(w+2)}}}\right)^{\left(a+\frac{1}{2}\right)} \times \sum_{m=0}^{K-1} C_{K-1}^m (-1)^m \times$$

$$\times (m+1)^{-\frac{1}{2}\left(a+\frac{5}{2}\right)} e^{\left(\frac{\alpha_2^2}{8b^2\lambda_{(w+2)}(m+1)}\right)} W_{-\frac{1}{2}(a+1/2),-\frac{1}{4}\left(\frac{\alpha_2^2}{4b^2\lambda_{(w+2)}(m+1)}\right)}. \tag{4.25}$$

The asymptotic expression as $Q \to +\infty$:

$$\text{OP}_{S_p}^{out,Q\to\infty} = \gamma\left(a+1, \frac{1}{b}\sqrt{\frac{\alpha_1}{\gamma_0}}\right) / \left(\Gamma(a+1)\right). \tag{4.26}$$

4.5 Simulation and discussion

Figure 4.2 shows the error metric $\xi_p(\%)$ in (24) versus term number of infinity sum (M) with the number $T \in \{7,10,15\}$. The results show that as the number of reflectors T increases, the number of M in (4.23) required to achieve a value close to the exact value will decrease.

From Fig 4.3 to Fig 4.6, we select $d_1 = d_2$ and $d_3 = d_4$. As the model is symmetric, the outage probabilities of the two secondary sources S_1 and S_2 have equal values.
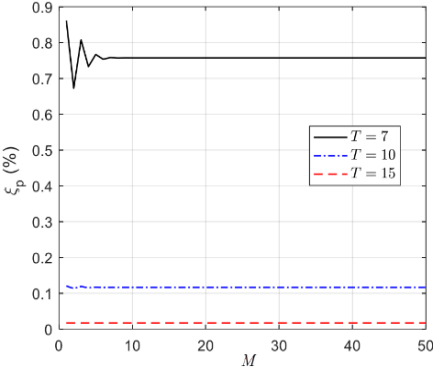

Figure 4.2: $\xi_p(\%)$ *versus M*
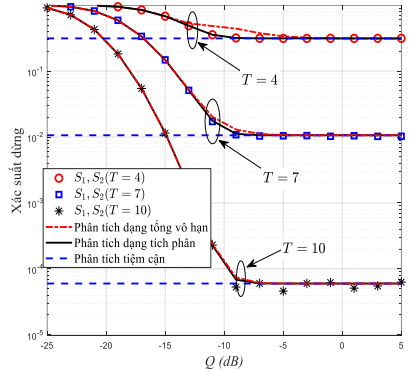
Figure 4.3: OP_{S_1} and OP_{S_2} *versus*
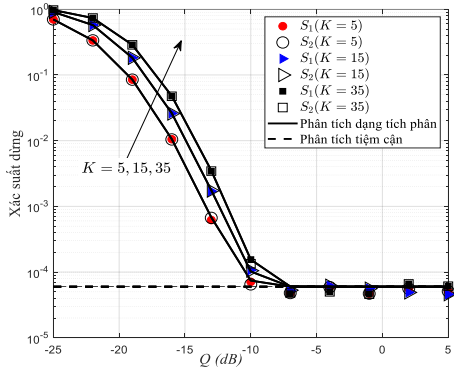
Fig 4.3 shows the OPs of two secondary sources versus $Q = I/N_0$ (dB). Fig. 3 exposes that in the small interference constraint parameter value region (between -25*dB* and -10*dB*), the OPs of both sources decrease when Q

13

increases, and in the high Q value region (over -10dB), the OPs reach a saturation value. The outage probabilities decrease as the number of metasurfaces T in the RIS increases. In Fig 4.3, the OP's analytic expressions are plotted as an infinite sum (using the first 25 terms) and integral form. When T increases the curves of the infinite sum formula get closer to the simulation line.

Fig 4.4 shows the OPs of two secondary sources versus $\gamma_0 = P_{max} / N_0(dB)$. The OPs of the two sources are the same because the coordinates of RIS and PR are chosen equidistant from the two sources, and the OP decreases as T increases. The OPs of the sources decrease rapidly as γ_0 rises between -25dB and −15dB, then fall into saturation due to the transmit power depending on a set of two parameters as in equation (4.1).
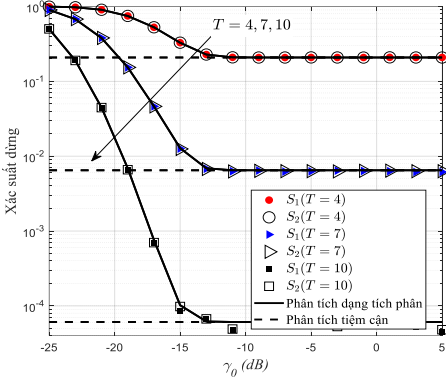
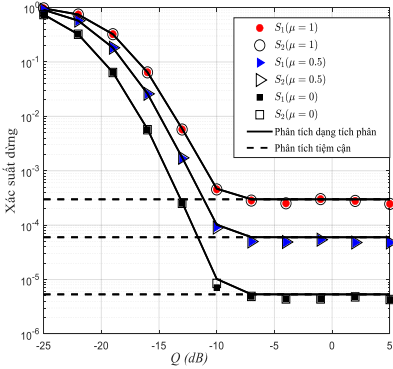**Figure 4.4:** OP_{S_1} *and* OP_{S_2} *versus* γ_0

**Figure 4.5:** OP_{S_1} and OP_{S_2} *versus* Q *(dB) when K changes*

Fig 4.5 shows the OPs of two secondary sources versus Q (dB) when the number of primary receiver changes. The results show that in the Q region less than -10dB, the number of PRs increases lead to the OPs of the secondary sources increase. When Q is greater than a threshold value (-10dB), the number of PRs no longer affects the performance of the secondary network.

Fig 4.6 shows the OPs of two secondary sources versus Q (dB) when the loop noise values are different. The results show that the increased loop noise will

increase the OPs of the secondary sources. And the OPs of the two secondary sources are the best for the perfect loop noise rejection case $\mu = 0$. The OPs also decrease as Q increases and reach saturation value when Q is large enough.

Figure 4.6: OP_{S_1} *and* OP_{S_2} *versus Q (dB) when* μ *changes.*
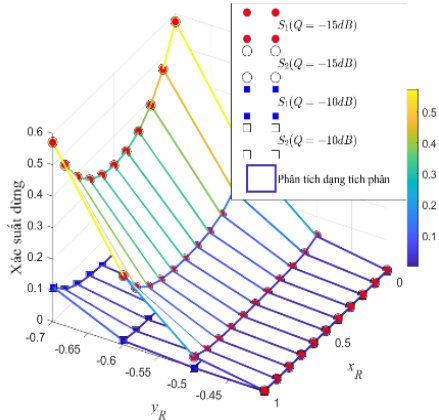
**Hình 4.7: Figure 4.7:** OP_{S_1} *and* OP_{S_2} *vesus* x_R *and* y_R.

Fig 4.7 shows the OPs of two secondary sources versus x_R and y_R. The results show that for the OPs of the sources are equal when the RIS is in locations with equal total distances from the RIS to the two sources. For the same y_R value, the RIS position equidistant from the two sources will give the smallest OP. Finally, for the same value of x_R, the OPs will decrease when y_R changing from -0.7 to -0.3.

Fig 4.8 illustrates the OPs of two secondary sources versus (x_{PR}, y_{PR}). The results show that when the primary receiver cluster is equidistant from the two sources, the OPs of the two sources are equal and the farther the primary receiver cluster is from the sources, the smaller the OPs are. When the primary receiver cluster is not equidistant from the two sources, the source closer to the primary receiver cluster will have the OPs smaller.

Fig 4.9 compares the outage probabilities of two secondary sources of the proposed MPR-UTW-RIS model with a two-way cooperative cognitive network model in duplex mode using AF relay. The results show that the

system with RIS supporting communication has much better performance than the system using AF relay even in the case of only one metasurface.
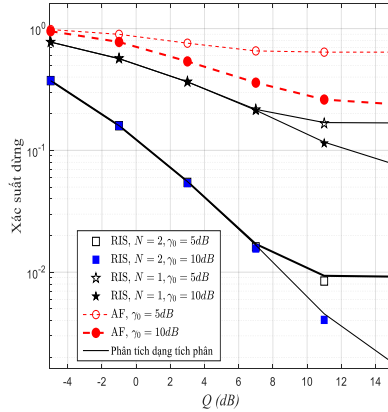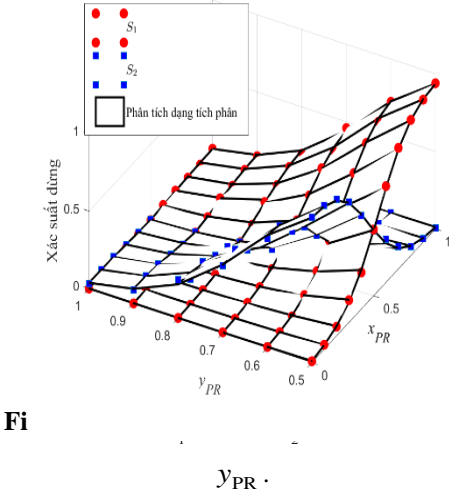
Figure 4.9: *Comparison of models using RIS and AF*

y_{PR} .

4.6 Conclusion

Chapter 4 proposes a two-way network model using reconfigurable intelligent surface in cognitive radio environments. The outage probabilities of two secondary sources are investigated according to many network parameters and the results show that the OPs are best when the RIS is equidistant from the two sources; the OPs decrease as the number of reflected elements increases, the distance between the primary receiver cluster and the two secondary sources increases, and as the loop noise decreases; and the OPs of the two secondary sources will reach saturation value when Q or γ_0 is large enough. Furthermore, the two-way system supported by the RIS has much smaller OPs of the secondary sources than the system supported by AF relay.

## Chapter 5. NONLINEAR ENERGY HARVESTING IN TWO-WAY COOPERATIVE NETWORKS

5.1 Introduction

In this chapter, a nonlinear energy harvesting (NEH) model is proposed for two-way cooperative networks. This model operates information transmission

in three time slots and uses the power splitting method of energy harvesting combined with digital network coding technique (DNC), called the NEH-TW-DNC protocol. The accurate and approximate expressions of the OPs of the sources are analyzed to evaluate the system performance. Furthermore, the author also compares the OPs of the sources between nonlinear energy harvesting and linear energy harvesting to observe the differences when considering real and ideal systems.

The contribution of chapter 5 is presented in the publication [P5].

5.2 System model
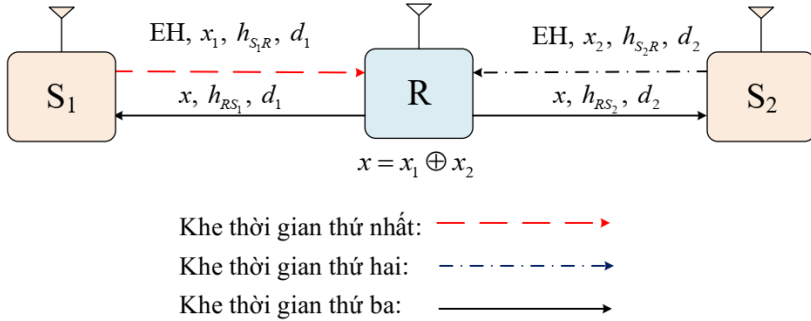
Figure 5.1: *System model NEH-TW-DNC*

Figure 5.1 depicts the two-way energy harvesting system model NEH-TW-DNC. The model consists of two sources S_1, S_2, and a relay R.

5.3 Signal transmission and signal-to-noise ratio

The operation process of the NEH-TW-DNC model is shown in Table 5.1. The signal-to-noise ratio (SNR) for decoding the signal x_1 and x_2 at the relay R in the first two time slots is:

$$\gamma_{S_1R} = (1-\rho)\left|h_{S_1R}\right|^2 P/N_0 = (1-\rho)\left|h_{S_1R}\right|^2 \gamma_0. \tag{5.2}$$

$$\gamma_{S_2R} = (1-\rho)\left|h_{S_2R}\right|^2 P/N_0 = (1-\rho)\left|h_{S_2R}\right|^2 \gamma_0. \tag{5.5}$$

The total harvested energy at the relay R can be calculated as follows:

$$E_h = \underset{\varsigma}{\eta \rho \alpha} \left(P_1 \left| h_{S_1 R} \right|^2 + P_2 \left| h_{S_2 R} \right|^2 \right) T \tag{5.7}$$

Because of the nonlinear EH, the transmit power of the relay device can be determined as follows:

$$P_R = \begin{cases} \varsigma \, P \left(\left| h_{S_1 R} \right|^2 + \left| h_{S_2 R} \right|^2 \right), & khi \quad P \left(\left| h_{S_1 R} \right|^2 + \left| h_{S_2 R} \right|^2 \right) \le P_{th}, \\ \varsigma P_{th}, & khi \quad P \left(\left| h_{S_1 R} \right|^2 + \left| h_{S_2 R} \right|^2 \right) > P_{th}, \end{cases} \tag{5.9}$$

Table 5.1: *The three-time slot transmission protocol of the NEH-TW-DNC mode.*

$S_1 \rightarrow R$	$S_2 \rightarrow R$	$R \rightarrow S_1, S_2$
NEH at Relay (ρ)	NEH at Relay (ρ)	$x = x_1 \oplus x_2$
Decoding signal x_1 from S_1	Decoding signal x_2 from S_2	Relay forwards signal x to sources
Time slot 1 αT	Time slot 2 αT	Time slot 3 $(1 - 2\alpha T)$
T		

The SNR required to decode the signal $x = x_1 \oplus x_2$ in the third time slot at the sources is:

$$\gamma_{RS_i} = \begin{cases} \dfrac{\left| h_{RS_i} \right|^2}{N_0} \varsigma \, P \left(\left| h_{S_1 R} \right|^2 + \left| h_{S_2 R} \right|^2 \right), & khi \quad P \left(\left| h_{S_1 R} \right|^2 + \left| h_{S_2 R} \right|^2 \right) \le P_{th}, \\ \dfrac{\left| h_{RS_i} \right|^2}{N_0} \varsigma P_{th}, & khi \quad P \left(\left| h_{S_1 R} \right|^2 + \left| h_{S_2 R} \right|^2 \right) > P_{th}. \end{cases} \tag{5.11}$$

From (5.2), (5.5) and (5.11), we have SNR to decode the signals x_1, x_2 at S_1, S_2, respectively:

$$\gamma_{S_1} = \min \left\{ \gamma_{S_2 R}, \gamma_{RS_1} \right\}, \ \gamma_{S_2} = \min \left\{ \gamma_{S_1 R}, \gamma_{RS_2} \right\}. \tag{5.12}$$

5.4 Performance analysis

The outage probability of S_1:

$$\text{OP}_{S_1} = \Pr\left[\gamma_{S_1} \leq \gamma_{th}\right] = \Pr\left[\gamma_{S_2 R} \leq \gamma_{th}\right] + \Pr\left[\gamma_{RS_1} \leq \gamma_{th}, \gamma_{S_2 R} > \gamma_{th}\right]. \tag{5.15}$$

After numerous complex calculations, we obtain the following results for the outage probability in two cases:

- Case 1: when $\lambda_1 = \lambda_2 = \lambda$:

$$\text{OP}_{S_1}\Big|_{\lambda_1 = \lambda_2 = \lambda} = 1 - e^{-(k_1/\lambda + k_3/\lambda_3)} + e^{-k_1/\lambda}\left(e^{-k_3/\lambda_3} - e^{-k 2/(k_1 \lambda_3)}\right) +$$

$$+ (\frac{k_1}{\lambda} - 1)\sum_{k=0}^{\infty} \frac{(-1)^k}{k!}\left(\frac{k_2}{\lambda \lambda_3}\right)^{k+1}\left[\Gamma\left(-k-1, \frac{k_1}{\lambda}\right) - \Gamma\left(-k-1, \frac{k_2}{k_3 \lambda}\right)\right] + \tag{5.20}$$

$$+ \sum_{k=0}^{\infty} \frac{(-1)^{k-1}}{k!}\left(\frac{k_2}{\lambda \lambda_3}\right)^{k+1}\left[\Gamma\left(-k, \frac{k_1}{\lambda}\right) - \Gamma\left(-k, \frac{k_2}{k_3 \lambda}\right)\right].$$

- Case 2: when $\lambda_1 \neq \lambda_2$:

$$\text{OP}_{S_1}\Big|_{\lambda_1 \neq \lambda_2} = 1 - e^{-(k_1/\lambda_2 + k_3/\lambda_3)} + e^{-k_1/\lambda_2}\left(e^{-k_3/\lambda_3} - e^{-k_2/(k_1 \lambda_3)}\right) +$$

$$+ \frac{\lambda_2}{(\lambda_1 - \lambda_2)}\sum_{k=0}^{\infty} \frac{(-1)^k}{k!}\left(\frac{k_2}{\lambda_2 \lambda_3}\right)^{k+1}\left[\Gamma\left(-k-1, \frac{k_1}{\lambda_2}\right) - \Gamma\left(-k-1, \frac{k_2}{k_3 \lambda_2}\right)\right] - \tag{5.21}$$

$$- \frac{\lambda_1 e^{-(1/\lambda_2 - 1/\lambda_1)k_1}}{(\lambda_1 - \lambda_2)}\sum_{k=0}^{\infty} \frac{(-1)^k}{k!}\left(\frac{k_2}{\lambda_1 \lambda_3}\right)^{k+1}\left[\Gamma\left(-k-1, \frac{k_1}{\lambda_1}\right) - \Gamma\left(-k-1, \frac{k_2}{k_3 \lambda_1}\right)\right].$$

Similarly, the outage probability of S_2 are found as (5.22) and (5.23) in the full-text thesis. When $P_{th} \to \infty$ we have the linear EH model

5.5 Simulation and discussion

In all figures the parameter is selected as: $\eta = 0.8$ $\alpha = 1/3$, $d_1 = 0.5$, $d_2 = 1 - d_1$. Figure 5.2 show the outage probabilities of two sources versus $P_s / N_0 (dB)$ with $P_{th} \in \{20, 40, \infty\} dB$. The results show that the OPs of two sources reduce when P_s / N_0 increases and saturates when P_s / N_0 is large enough. The values of the saturation OP differ and depend on the values of P_{th}, if P_{th} increases, the values the saturation OP decrease. Besides, when $P_s / N_0 < P_{th}$ leads to $\text{OP}_{S_1} > \text{OP}_{S_2}$ and when $P_s / N_0 > P_{th}$ leads to $\text{OP}_{S_1} < \text{OP}_{S_2}$. When $P_s / N_0 < P_{th}$, the

OPs of each source in the two cases of nonlinear EH and linear EH are approximately equal, In contrast, when $P_s / N_0 > P_{th}$, the OPs reach saturation in case of nonlinear EH and the OPs continue to decrease in case of linear EH, as P_s / N_0 increases. Finally, the OP curves of nonlinear EH approach those of linear EH as $P_{th} \to \infty$.
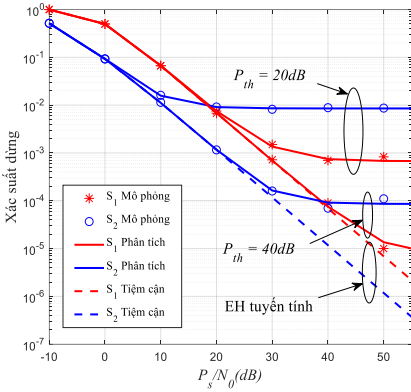
**Figure 5.2:** OP_{S_1}, OP_{S_2} *versus* $P_s / N_0 (dB)$
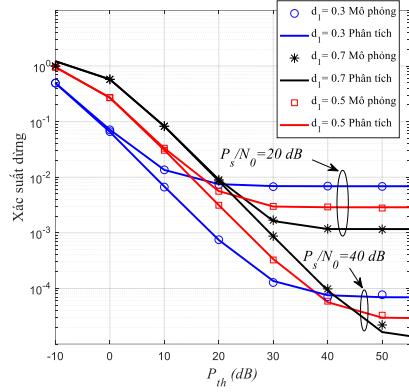
Figure 5.3: OP_{S_1} *versus* $P_{th} (dB)$

Figure 5.3 represents the outage probabilities of the source S_1 as a function of $P_{th} (dB)$ with two values of P_s / N_0 and three values of d_1. The results indicate that the OP_{S_1} decreases as P_{th} increases and P_s / N_0 decreases. The OP_{S_1} reaches a saturation value when P_{th} increases to a sufficiently large value, and this value varies depending on the values of P_s / N_0 and d_1. Additionally, when $P_{th} < P_s / N_0$, the d_1 is smaller as OP_{S_1} is smaller. Conversely, when $P_{th} > P_s / N_0$, the d_1 is larger as OP_{S_1} is smaller. Figure 5.4 illustrates the OP_{S_1} as a function of ρ with
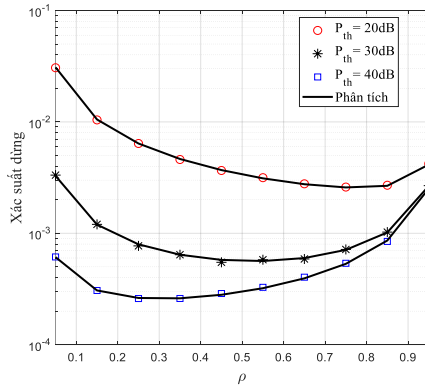
Figure 5.4: OP_{S_1} *versus* ρ

$P_s / N_0 = 30 (dB)$, $P_{th} \in \{20, 30, 40\} dB$. The results show that the OP_{S_1} decreases as P_{th} increases. Moreover, for each set of parameters, there is always a value of ρ so that the source has the smallest outage probability.

5.6 Conclusion

Chapter 5 investigates a two-way cooperative network with nonlinear energy harvesting at the relay. As the threshold power for saturation of the nonlinear energy harvesting at the relay increases, the outage probabilities of the sources decrease. The outage probabilities reach a saturation value when P_s / N_0 and P_{th} are sufficiently large. For each set of parameters, there exists an optimal power allocation coefficient that minimizes the outage probability.

Chapter 6. CONCLUSION

4.1 The results of the thesis

The dissertation investigated techniques and protocols to enhance the communication performance of the two-way cooperative networks in conventional wireless and cognitive wireless systems. The proposed models have considered both ideal conditions and practical constraints to provide a more comprehensive evaluation of the system. The new contributions and key results of the thesis are as follows:

Firstly, the successful proposal and analysis of a two-way cooperative network model incorporating the combination of relay cluster, successive interference cancellation technique, and digital network coding technique. The model was examined under both ideal conditions and real conditions, such as imperfect successive interference cancellation and imperfect channel state information. The research results demonstrate that the system throughput of the SIC-2TS protocol outperforms protocols that do not utilize the combination of these techniques. Additionally, the proposed partial relay selection scheme helps reduce the collection time of imperfect channel state information compared to other relay selection methods, thereby reducing signal processing time and

increasing transmission speed. The effectiveness of spatial diversity increases, and the outage probability decreases as the number of relays in the cluster increases. The research results also highlight the significant impact of non-ideal conditions (ipSIC/ipCSI) on the system performance. Furthermore, when the relay cluster is placed at optimal positions and the power allocation coefficients are properly determined, the two sources can achieve the best performance.

Next, the successful proposal and analysis of a two-way network model utilizing a reconfigurable intelligent surface in cognitive radio environments. The model operates in a full-duplex mode and investigates real conditions where residual interference exists after interference cancellation at the receiving antenna, and the secondary network is power-limited due to multiple primary receivers. The objective of the model is to reduce the outage probability, increase spectrum efficiency, energy efficiency, and cost-effectiveness of the TW network. The OPs of the secondary sources were investigated based on various network parameters, and the results show the following: The best OP is achieved when the RIS is equidistant from the two sources; The OPs decrease when the number of reflecting elements in the RIS increases, the distances between the primary receivers and the secondary sources increase, and the loop interference decreases; The OPs reach a saturation state when the maximum interference power to plus noise ratio that PUs can decode information in the primary network or the maximum transmit power that the hardware of the secondary sources can handle at a sufficiently large. Moreover, the system performance of the two-way network with the RIS-aided is better than the similar network with the AF relay-aided.

Chapter 5 proposes and analyzes a two-way cooperative network model with nonlinear energy harvesting at the DF relay. The model considers the fact that the energy collector of the relay is made of nonlinear electronic components. The model uses power division energy harvesting and digital network coding techniques. The proposal's contribution is to use green energy from radio waves to support signal transmission for low-cost and resource-constrained networks such as wireless sensor networks and IoT systems. The results show that for

each set of system parameters, it is possible to determine the optimal power allocation factor so that the OP is the smallest.

All performance evaluation parameters of the proposals in the thesis are analyzed in the form of explicit expressions and the results of mathematical analysis are verified by the Monte Carlo simulation method. The results of the research project can make useful contributions to the research community, to companies manufacturing telecommunications equipment, towards providing better service quality to customers. The proposed models of the thesis can be used in IoT networks, heterogeneous networks, wireless sensor networks, industrial robotics networks. The research results in the thesis have been published in prestigious SCIE journals and international conferences.

4.2 Development direction of the thesis

The dissertation has made proposals with results to achieve the set objectives. However, in today's context, with the increasing number of wireless communication applications and the growing demand for high-quality wireless services, the goal of improving network performance in applications and specific conditions remains an important issue to address. In the future, the author will continue to focus on enhancing the performance of two-way networks, such as improving spectrum efficiency, energy efficiency, and transmission speed for two-way cooperative networks in conventional wireless networks and cognitive wireless networks. Additionally, the research will consider more realistic operating conditions. The specific research plans are as follows:

- Consider two-way networks studied in other fading channels such as Nakagami-m, Rician, double Rayleigh channels.
- Investigate nonlinear EH two-way cooperative network model with direct transmission.
- Performance evaluation in terms of reliability and latency of studied bidirectional networks using short packets.

- Design deep learning networks from analysis and simulation data to predict two-way system performance.

- Research on hybrid networks between two-way terrestrial networks and satellite networks.